Chemical Engineering Journal 388 (2020) 124226

Contents lists available at ScienceDirect

Chemical Engineering Journal

journal homepage: www.elsevier.com/locate/cej

Freezing-enhanced non-radical oxidation of organic pollutants by peroxymonosulfate

Nhat Thi Hong Le[a], Jinjung Ju[a], Bomi Kim[b,c], Min Sik Kim[d], Changha Lee[e], Saewung Kim[f], Wonyong Choi[g], Kitae Kim[b,c,*], Jungwon Kim[a,f,*]

[a] Department of Environmental Sciences and Biotechnology, Hallym University, Chuncheon, Gangwon-do 24252, Republic of Korea
[b] Korea Polar Research Institute (KOPRI), Incheon 21990, Republic of Korea
[c] Department of Polar Sciences, University of Science and Technology (UST), Incheon 21990, Republic of Korea
[d] Department of Chemical and Environmental Engineering, Yale University, New Haven, CT 06511, United States
[e] School of Chemical and Biological Engineering, Institute of Chemical Process (ICP), Seoul National University, Seoul 08826, Republic of Korea
[f] Department of Earth System Science, University of California, Irvine, Irvine, CA 92697, United States
[g] Division of Environmental Science and Engineering, Pohang University of Science and Technology (POSTECH), Pohang 37673, Republic of Korea

HIGHLIGHTS

- Degradation of aquatic pollutants by PMS is significantly accelerated by freezing.
- Both PMS and pollutants are concentrated in the ice grain boundaries.
- Enhanced degradation in frozen solution is due to the freeze-concentration effect.
- Degradation occurs through the direct electron transfer from pollutants to PMS.
- The PMS/freezing system is an eco-friendly water treatment method.

GRAPHICAL ABSTRACT

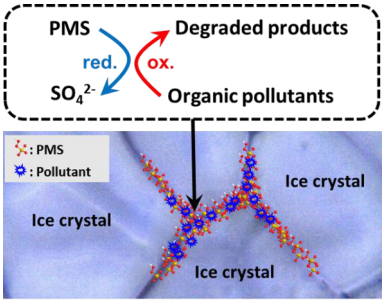

ARTICLE INFO

Keywords:
Peroxymonosulfate
Freeze-concentration effect
Redox chemical reaction
Non-radical mechanism
Pharmaceutical pollutant

ABSTRACT

This study presents a freezing method for accelerating the peroxymonosulfate (PMS)-mediated degradation process. The degradation of furfuryl alcohol (FFA) in the presence of PMS was markedly accelerated by freezing. The degradation efficiency of FFA was only 10.4% in aqueous solution at 25 °C, but 100% degradation was achieved in frozen solution at −20 °C after 3 h of reaction at [FFA] = 20 μM and [PMS] = 100 μM. This accelerated PMS-mediated degradation of FFA in the frozen solution is due to the concentration of both PMS and FFA in ice grain boundaries, which increases the collision frequency between PMS and FFA thereby facilitating redox transformation. The mapping images of PMS and FFA in the frozen sample obtained using confocal Raman microscopy provide clear evidence of the accumulation of PMS and FFA in the ice grain boundaries after freezing. The experimental results with sulfate radical ($SO_4^{\cdot -}$) scavengers, no production of hydroxyl radicals ($^{\cdot}OH$) and $SO_4^{\cdot -}$, and the highly pollutant-dependent degradation efficiency suggest that the PMS-mediated degradation in frozen solution primarily proceeds through the direct electron transfer from organic pollutants to PMS (non-radical mechanism) rather than the reaction of $SO_4^{\cdot -}$ or $^{\cdot}OH$ with organic pollutants (radical mechanism). The degradation efficiency of the PMS/freezing system was similar across the pH range of 3–10. In addition, the PMS/freezing system worked efficiently in the temperature range of −10 to −35 °C. This result implies that the PMS/freezing system can be operated without external energy in cold regions.

* Corresponding authors at: Korea Polar Research Institute (KOPRI), Incheon 21990, Republic of Korea (K. Kim). Department of Environmental Sciences and Biotechnology, Hallym University, Chuncheon, Gangwon-do 24252, Republic of Korea (J. Kim).
E-mail addresses: ktkim@kopri.re.kr (K. Kim), jwk@hallym.ac.kr (J. Kim).

https://doi.org/10.1016/j.cej.2020.124226
Received 20 November 2019; Received in revised form 10 January 2020; Accepted 25 January 2020
Available online 28 January 2020
1385-8947/

1. Introduction

Peroxymonosulfate (PMS) has a thermodynamically high oxidation power with a reduction potential of 1.19 V_{NHE} for one-electron transfer ($E^0(HSO_5^-/SO_4^{\cdot -})$) [1] and 1.75 V_{NHE} for two-electron transfer ($E^0(HSO_5^-/SO_4^{2-})$) [2]. However, the reaction of PMS with aquatic pollutants is kinetically very slow, which limits the practical applications of PMS as a chemical oxidant for water treatment [3].

To overcome the drawback of PMS-mediated oxidation (i.e., the low reactivity of PMS toward aquatic pollutants), a variety of techniques have been employed to convert PMS to more reactive species such as hydroxyl radicals ($^{\cdot}OH$, $E^0(^{\cdot}OH/OH^-) = 1.77\ V_{NHE}$) [4] and sulfate radicals ($SO_4^{\cdot -}$, $E^0(SO_4^{\cdot -}/SO_4^{2-}) = 2.43\ V_{NHE}$) [5], including heat [6], ultrasound [7], UV light [8,9] (reaction (1)), transition metal ion [10,11], and metal oxide [12–14]-induced activation of PMS (reaction (2)). The oxidative degradation of aquatic pollutants rapidly proceeds by $SO_4^{\cdot -}$ and/or $^{\cdot}OH$ generated from PMS activation (radical mechanism).

$$HSO_5^- + \text{heat, ultrasound, or UV light} \rightarrow SO_4^{\bullet -} + {}^{\bullet}OH \quad (1)$$

$$M^{n+} + HSO_5^- \rightarrow M^{(n+1)+} + SO_4^{\bullet -} + OH^- \quad (2)$$

It has also been reported that PMS can rapidly oxidize aquatic pollutants in the presence of noble metals [15], carbon nanotubes [16,17], and graphitized nanodiamonds [18] as electron mediators through a non-radical mechanism. The complexation between PMS and electron mediators enhances pollutant degradation without radical involvement by facilitating electron transfer from pollutants to electron mediator/PMS complexes (reaction (3)).

$$\text{pollutant} + \text{electron mediator/PMS complex} \rightarrow \text{pollutant}^+ + \text{electron mediator/PMS}^- \text{ complex} \quad (3)$$

Chemical reactions in the ice phase at temperatures below the freezing point are usually slower than those in the aqueous phase at temperatures above the freezing point. However, some chemical reactions in the ice phase occur faster than those in the aqueous phase because of the solute concentration and the pH change during freezing, the so-called freeze-concentration effect [19,20]. Both solid (ice crystals) and liquid phases (ice grain boundaries, which are the liquid regions between ice crystals) exist below the freezing point. Solutes are gradually accumulated in the ice grain boundaries during freezing as ice crystals grow [21]. The pH of acidic solutions decreases but the pH of basic solutions increases by freezing, because protons and hydroxides are accumulated in the ice grain boundaries under acidic and basic conditions, respectively [22]. The concentration of solutes and protons (or hydroxides) in the ice grain boundaries during freezing increases the reaction probability between solutes and converts some solutes to more reactive species through protonation (or deprotonation) [23]. Based on the freeze-concentration effect, freezing methods have been recently developed to enhance the oxidative degradation of various organic pollutants, such as sulfamethoxazole (oxidant: nitrite (NO_2^-)) [24], phenolic pollutants (oxidant: chromate ($HCrO_4^-$)) [25], waste-activated sludge (oxidant: NO_2^-) [26], and pharmaceutical pollutants (oxidant: periodate (IO_4^-)) [27]. However, there are two issues in these freezing systems that limit their practical applications for water treatment: the restricted pH working range and the generation of toxic ions such as nitrate (NO_3^-), trivalent chromium (Cr^{3+}), and iodide (I^-, which can induce the formation of toxic iodinated organic compounds in the disinfection process [28,29]).

In this study, PMS was used as an oxidant in the freezing-induced water treatment system to prevent the problems observed in the freezing systems for water treatment previously reported. Although various methods to enhance the PMS-mediated oxidation process have been extensively studied, the freezing method has not been tried. The degradation of furfuryl alcohol (FFA, as a model organic compound) by PMS in frozen solution at −20 °C was compared with that in aqueous solution at 25 °C. Products generated from the reduction of PMS in frozen solution were identified and the mechanism of PMS-mediated degradation in frozen solution was investigated. The degradation kinetics of FFA in the PMS/freezing system was also measured as a function of various experimental parameters. Furthermore, the practical viability of the PMS/freezing system was discussed based on its degradation efficiencies for a variety of organic pollutants (pharmaceutical and phenolic pollutants) and in repeated degradation cycles.

2. Chemicals and methods

2.1. Chemicals

All chemicals were of high-purity grade and used as received without further purification. They include potassium peroxymonosulfate (PMS, $KHSO_5{\cdot}0.5KHSO_4{\cdot}0.5K_2SO_4$, Sigma-Aldrich), furfuryl alcohol (FFA, $C_5H_6O_2$, Sigma-Aldrich, ≥98.0%), tryptophan ($C_{11}H_{12}N_2O_2$, Sigma-Aldrich, ≥98.0%), propranolol hydrochloride ($C_{16}H_{21}NO_2{\cdot}HCl$, Sigma-Aldrich, ≥99.0%), sulfamoxole ($C_{11}H_{13}N_3O_3S$, Fluka, ≥98.0%), sulfamethoxazole ($C_{10}H_{11}N_3O_3S$, Fluka, analytical standard), phenol (C_6H_5OH, Sigma-Aldrich, ≥99.0%), 4-methylphenol ($CH_3C_6H_4OH$, Sigma-Aldrich, analytical standard), bisphenol A ($((CH_3)_2C(C_6H_4OH)_2$, Sigma-Aldrich, ≥99.0%), methanol (CH_3OH, Wako, ≥99.8%), 2-propanol ($(CH_3)_2CHOH$, Sigma-Aldrich, ≥99.5%), benzene (C_6H_6, Sigma-Aldrich, ≥99.9%), benzoic acid (C_6H_5COOH, Sigma-Aldrich, ≥99.5%), coumarin ($C_9H_6O_2$, Sigma, ≥99.0%), 5-tert-butoxycarbonyl-5-methyl-1-pyrroline-*N*-oxide (BMPO, $C_{10}H_{17}NO_3$, ENZO Life Sciences, ≥99.0%), iron(II) perchlorate hydrate ($Fe(ClO_4)_2{\cdot}xH_2O$, Sigma-Aldrich, ≥98.0%), cobalt(II) perchlorate hexahydrate ($Co(ClO_4)_2{\cdot}6H_2O$, Sigma-Aldrich, ≥98.0%), phosphoric acid (H_3PO_4, Junsei, 85%), acetonitrile (CH_3CN, J.T. Baker, ≥99.9%), sodium carbonate (Na_2CO_3, Sigma-Aldrich, ≥99.5%), and sodium bicarbonate ($NaHCO_3$, Sigma-Aldrich, ≥99.7%). All solutions were prepared in ultrapure deionized water (18.3 MΩ·cm) produced by a Human-Power I + water purification system (Human Corporation).

2.2. Experimental procedure

Aliquots of PMS (usually 1 mM, 10 mL) and an organic pollutant (usually FFA, 200 μM, 10 mL) stock solution were added to water (usually 80 mL) in a beaker to yield the desired initial concentration (usually [PMS] = 100 μM and [organic pollutant] = 20 μM). The aqueous solution pH was adjusted by concentrated perchloric acid ($HClO_4$) or sodium hydroxide (NaOH) solution to the desired value (usually pH 3.0). Ten mL of sample solution was put in a polypropylene conical tube (volume = 15 mL, Corning), which was then immersed into an ethanol-circulated bath. Ethanol, used as a coolant, was cooled to the desired temperature (usually −20 °C) before immersing the conical tube. Several conical tubes containing the same sample solution (usually 7 conical tubes) were put into the ethanol-circulated bath at a time. The reaction time was started from the moment the conical tube containing the aqueous sample was immersed into the ethanol-circulated bath. The frozen samples in the ethanol-circulated bath were withdrawn one by one at fixed time intervals (usually 10, 20, 30, 60, 120, 180, and 240 min) and thawed in a lukewarm water bath at 35 °C for sample analysis. The aqueous sample was then immediately analyzed.

Experiments in the ethanol-circulated bath preset at 25 °C were performed as controls. Aqueous reactions in the presence of ice pellets were also performed as a control. Briefly, the aqueous solution (5 mL and pH 3.0) containing PMS (200 μM) and FFA (40 μM) was cooled to 4 °C. Ice pellets (5 g and pH 3.0) were added into the aqueous solution of PMS and FFA, which was considered as the reaction start time. The aqueous reactions with ice pellets proceeded at 4 °C in a refrigerator to inhibit the ice pellets melting. All experiments were performed in duplicate or triplicate to confirm data reproducibility.

2.3. Chemical analyses

The concentrations of organic pollutants, such as FFA, tryptophan, propranolol, sulfamoxole, sulfamethoxazole, phenol, 4-methylphenol, and bisphenol A, were analyzed using a high-performance liquid chromatograph (HPLC, Agilent 1120) equipped with a UV–visible detector and a Zorbax 300SB C-18 column (4.6 mm × 150 mm). The eluent consisted of a binary mixture of phosphoric acid solution (0.1%) and acetonitrile. The volume ratios (0.1% phosphoric acid solution: acetonitrile) of the eluents and the detection wavelengths were as follows: 85:15 and 218 nm for FFA, 90:10 and 273 nm for tryptophan, 50:50 and 291 nm for propranolol, 90:10 and 267 nm for sulfamoxole, 80:20 and 265 nm for sulfamethoxazole, 70:30 and 270 nm for phenol, 75:25 and 280 nm for 4-methylphenol, and 70:30 and 229 nm for bisphenol A, respectively. Quantitative analysis of sulfate (SO_4^{2-}) was performed using an ion chromatograph (IC, Dionex DX-120) equipped with a conductivity detector and a Dionex IonPac AS-14 column (4 mm × 250 mm). The eluent was a binary mixture of sodium carbonate (3.5 mM) and sodium bicarbonate (1 mM), and its flow rate was 1.0 mL/min.

To determine whether $SO_4^{\cdot -}$ is generated or not in the PMS/freezing system, electron paramagnetic resonance (EPR) analysis was performed. 5-tert-butoxycarbonyl-5-methyl-1-pyrroline-*N*-oxide (BMPO, 1 mM) was used as a spin-trapping reagent of $SO_4^{\cdot -}$ [30]. The EPR spectra were obtained using an electron paramagnetic resonance spectrometer (JEOL JES-TE300) under the following conditions: microwave power = 1 mW, microwave frequency = 9.415 GHz, center field = 3354 G, modulation width = 0.2 mT, and modulation frequency = 100 kHz. The production of $^{\cdot}OH$ was verified by measuring the fluorescence emission intensity of 7-hydroxycoumarin that was generated from the reaction between $^{\cdot}OH$ and coumarin ($^{\cdot}OH$ + coumarin → 7-hydroxycoumarin) [31]. Monochromatic light with a wavelength of 332 nm was used as the excitation source and the fluorescence emission intensity was monitored at 460 nm using a spectrofluorometer (Shimadzu RF-5301).

The spatial distributions of PMS and FFA in frozen solution were investigated using a confocal Raman microscope (Renishaw inVia Qontor). The glass sample holder (8 mm × 8 mm × 2 mm) was loaded with 100 μL of aqueous PMS solution at [PMS] = 100 μM and pH 3.0 (or aqueous FFA solution at [FFA] = 10 mM and pH 3.0) and mounted on a temperature-controlled microscope stage (Linkam Scientific THMS600). The temperature was decreased from 0 to −20 °C at a rate of −1.5 °C/min. A monochromatic laser with a wavelength of 532 nm was used as the excitation source. Chemical mapping images of PMS and FFA were obtained by measuring the emission intensity at 942 cm^{-1} and 1504 cm^{-1}, respectively.

3. Results and discussion

3.1. Degradation of FFA by PMS in aqueous and frozen solutions

To compare the degradation capacities of PMS in frozen and aqueous solutions, FFA was selected as a model organic compound [27,32,33], and its degradation kinetics in the presence of PMS was measured at −20 °C for ice phase reactions and 25 °C for aqueous phase reactions (Fig. 1). The degradation of FFA by PMS in aqueous solution was very slow, whereas it proceeded rapidly in frozen solution. The degradation efficiency of FFA in aqueous solution was only 10.4% after 3 h of reaction. However, 85.9% of FFA was degraded after 1 h and complete degradation was achieved after 3 h in frozen solution. The negligible degradation of FFA without PMS implies that PMS acts as the sole oxidant for the degradation of FFA.

The oxidative degradation of FFA by PMS should be accompanied by the reductive transformation of PMS by FFA. Therefore, we investigated the anionic products generated from the reduction of PMS by FFA during freezing using an ion chromatograph. The concentration of sulfate (SO_4^{2-}) gradually increased with reaction time, but the production of other anions was below the detection limit. When the degradation of FFA was complete (after 3 h of reaction), the generation of SO_4^{2-} was almost absent. This result confirms that the degradation of FFA proceeds through the redox chemical reaction between PMS and FFA in frozen solution.

In the IO_4^-/freezing system, I^- is generated from the reduction of IO_4^- by organic pollutants in frozen solution ($IO_4^- + 2H^+ + 2e^- \rightarrow IO_3^- + H_2O$; $IO_3^- + 6H^+ + 6e^- \rightarrow I^- + 3H_2O$) [27]. I^- can act as a precursor of highly toxic and carcinogenic iodinated organic compounds in natural systems [34,35] and in the oxidation process using free chlorine or manganese dioxide [28,29]. This behavior restricts the use of IO_4^- in environmental remediation. Both the $HCrO_4^-$/freezing system and NO_2^-/freezing system for water treatment have similar problems [24–26]. However, the reduction of PMS by FFA induces the formation of only SO_4^{2-}, which has negligible toxicity [36,37] and acts as nutrient to plants [38,39]. Therefore, the PMS/freezing system can be proposed as an eco-friendly method for the degradation of aquatic pollutants.

The degradation of FFA by PMS in frozen solution occurs through the direct electron transfer from FFA to PMS (reactions (4)–(7), non-radical mechanism). The direct electron transfer from FFA to PMS (more precisely, the electrophilic peroxo oxygen in PMS) generates oxidation intermediates such as furfural and 2-furoic acid [40], and the subsequent electron transfer from intermediates to PMS leads to the generation of ring-opened products and carbon dioxide. In addition, if the one-electron reduction of PMS by FFA is possible during freezing, $SO_4^{\cdot -}$ is generated from reaction (7) and the radical mechanism can also be involved in the degradation process (reaction (8)).

$$HSO_5^- + 2H^+ + 2e^-(\text{from FFA}) \rightarrow HSO_4^- + H_2O \quad (4)$$

$$HSO_5^- + H^+ + 2e^-(\text{from FFA}) \rightarrow SO_4^{2-} + H_2O \quad (5)$$

$$SO_5^{2-} + H_2O + 2e^-(\text{from FFA}) \rightarrow SO_4^{2-} + 2OH^- \quad (6)$$

$$HSO_5^- + e^-(\text{from FFA}) \rightarrow SO_4^{\cdot -} + OH^- \quad (7)$$

$$SO_4^{\cdot -} + e^-(\text{from FFA}) \rightarrow SO_4^{2-} \quad (8)$$

To determine which mechanism is dominant (non-radical mechanism vs. radical mechanism), the degradation of FFA by PMS in frozen solution was examined in the presence of various $SO_4^{\cdot -}$ scavengers with different bimolecular rate constants toward $SO_4^{\cdot -}$ (k) (Fig. 2). Methanol (k = 1.0–1.1 × 10^7 M^{-1} s^{-1}), 2-propanol (k = 7.9–8.2 × 10^7 M^{-1} s^{-1}), benzoic acid (k = 1.2 × 10^9 M^{-1} s^{-1}), and benzene (k = 2.4 × 10^9 M^{-1} s^{-1}) [41–44] were used as $SO_4^{\cdot -}$ scavengers. The effects of all $SO_4^{\cdot -}$ scavengers on the degradation of FFA were negligible or small despite a much higher concentration of

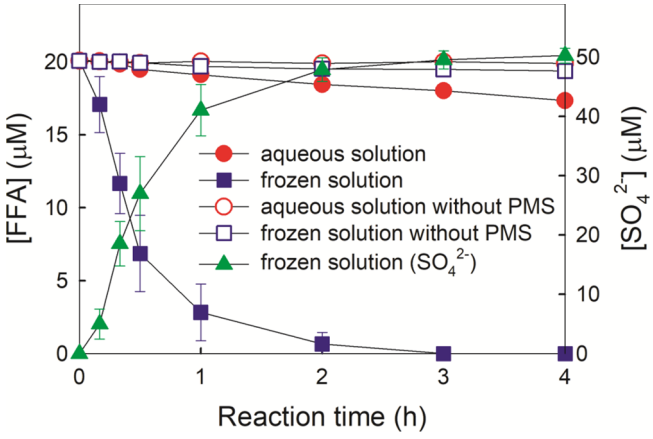

Fig. 1. Degradation of FFA by PMS in aqueous and frozen solutions. Experimental conditions: [PMS] = 100 μM, [FFA] = 20 μM, pH 3.0, and reaction temperatures = 25 °C for aqueous phase reactions and −20 °C for ice phase reactions.

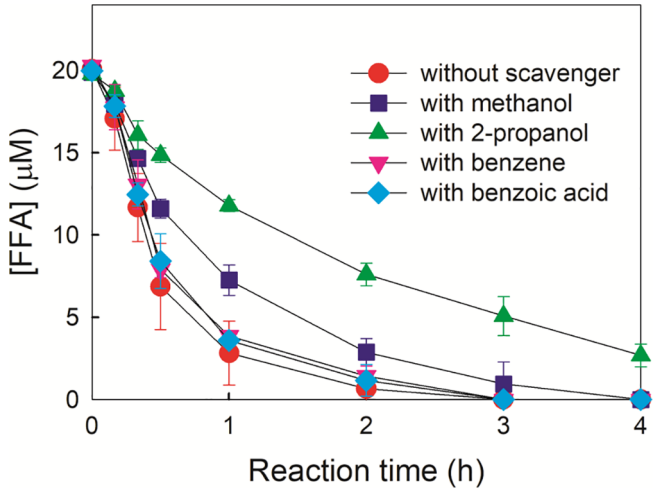

Fig. 2. Effects of sulfate radical ($SO_4^{\cdot -}$) scavengers on the PMS-mediated degradation of FFA in frozen solution. Experimental conditions: [PMS] = 100 μM, [FFA] = 20 μM, [methanol] = [2-propanol] = [benzene] = [benzoic acid] = 1 mM, pH 3.0, and reaction temperature = −20 °C for ice phase reactions.

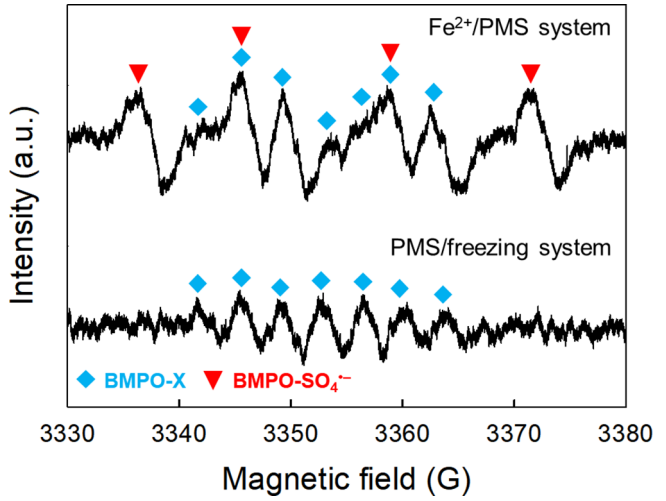

Fig. 3. EPR spectra obtained in the Fe^{2+}/PMS system and the PMS/freezing system. Experimental conditions: [PMS] = 100 μM, [FFA] = 20 μM, [Fe^{2+}] = 20 μM for the Fe^{2+}/PMS system, [BMPO] = 1 mM, pH 3.0, reaction time = 0.5 h, and reaction temperatures = 25 °C for the Fe^{2+}/PMS system and −20 °C for the PMS/freezing system.

$SO_4^{\cdot -}$ scavengers (1 mM) than FFA (20 μM). The slight decrease of FFA degradation in the presence of methanol or 2-propanol seems to be due to the direct reaction of PMS with $SO_4^{\cdot -}$ scavenger. In addition, the inhibitory effect of $SO_4^{\cdot -}$ scavengers on the degradation of FFA was not related to their reactivity toward $SO_4^{\cdot -}$ (k values). The reactivities of $SO_4^{\cdot -}$ scavengers toward $SO_4^{\cdot -}$ are in the order benzene > benzoic acid > 2-propanol > methanol; however, their inhibitory effects were in the order 2-propanol > methanol > benzene ≈ benzoic acid. These results imply that even though reaction (7) is possible, $SO_4^{\cdot -}$ generated from reaction (7) (i.e., the radical mechanism) has a negligible effect in the PMS-mediated degradation process in frozen solution.

To confirm the non-radical mechanism as the primary degradation pathway in the PMS/freezing system, the production of $SO_4^{\cdot -}$ in the PMS/freezing system and the Fe^{2+}/PMS system (as a control) was monitored in the presence of BMPO using EPR spectroscopy (Fig. 3). The characteristic peaks of BMPO–$SO_4^{\cdot -}$ adduct appeared in the EPR spectrum of the Fe^{2+}/PMS system, which is consistent with the previous results [45,46]. However, only the EPR signal corresponding to 5-tert-butoxycarbonyl-5-methyl-2-oxo-pyrroline-1-oxyl (BMPO–X), which is a product generated from the direct oxidation of BMPO [30], was observed in the PMS/freezing system. This result indicates that reaction (7) (i.e., the generation of $SO_4^{\cdot -}$) is not favored, and therefore, reactions (4)–(6) (two-electron transfer processes) can be proposed as the primary degradation pathways in the PMS/freezing system.

We also investigated the production of 7-hydroxycoumarin (coumarin–OH adduct) from coumarin, which is proportional to $^{\cdot}OH$ generation [47,48] (Fig. 4). If $SO_4^{\cdot -}$ is generated from reaction (7) (one-electron transfer process), $^{\cdot}OH$ is inevitably generated because $SO_4^{\cdot -}$ can react with water molecules and hydroxide ions ($SO_4^{\cdot -} + H_2O \rightarrow SO_4^{2-} + H^+ + {}^{\cdot}OH$ ($k < 3.0 \times 10^3\ s^{-1}$) and $SO_4^{\cdot -} + OH^- \rightarrow SO_4^{2-} + {}^{\cdot}OH$ ($k = 6.5 \times 10^7\ M^{-1}\ s^{-1}$)) [49,50]. In accordance with previous studies [51,52], the Co^{2+}/PMS system produced a significant level of 7-hydroxycoumarin (i.e., $^{\cdot}OH$) through reaction (7) (one-electron transfer from Co^{2+} to PMS) and the subsequent reaction of $SO_4^{\cdot -}$ with H_2O or OH^-. However, the production of 7-hydroxycoumarin (i.e., $^{\cdot}OH$) was negligible in the PMS/freezing system at both pH 3.0 and 10.0. No production of $^{\cdot}OH$ in the PMS/freezing system reconfirms that the direct electron transfer process from organic pollutants to PMS (non-radical mechanism) is primarily responsible for the degradation of organic pollutants in the PMS/freezing system.

3.2. Concentration of PMS and FFA in the ice grain boundaries by freezing

The concentrations of the solutes in the ice phase (more precisely, in the ice grain boundaries) are higher than those in the aqueous phase because the solutes are excluded from the ice crystals and accumulated in the ice grain boundaries during freezing. It has been estimated that the concentrations of methylene blue increase by approximately 10^3 times at 77 K and 10^6 times at 243 K, respectively, compared to those at temperatures above the freezing point [21]. The accelerated PMS-mediated degradation of FFA in frozen solution is most likely due to the increase in both PMS and FFA concentrations during freezing. This freeze-concentration effect can increase the reaction probability between PMS and FFA and therefore accelerate the degradation of FFA by PMS.

To provide direct evidence for the accumulation of PMS in the ice grain boundaries after freezing, the Raman spectra of PMS in ice crystals and ice grain boundaries were measured in the frozen sample without thawing (Fig. 5). Fig. 5a shows the optical image of the frozen PMS solution where the presence of ice grain boundaries is clearly observed between ice crystals, ranging in size from 5 to 10 μm. The characteristic Raman PMS peaks were observed in the ice grain boundary region (site marked with red circle in Fig. 5a). Multiple peaks in the 600–650 cm^{-1} and 900–950 cm^{-1} regions are assigned to O = S = O bending modes and symmetric/asymmetric S − O stretching modes, respectively. Two peaks at 1088 and 1126 cm^{-1} are ascribed to S = O stretching [53–55]. However, any Raman peaks were not observed in the ice crystal region (site marked with blue circle in Fig. 5a) (Fig. 5b). Fig. 5c shows the PMS mapping image of the frozen PMS solution, which was obtained by measuring the emission intensity at 942 cm^{-1} under excitation at 532 nm using a confocal Raman microscope. The relative concentrations of PMS are displayed on a rainbow scale (black and violet: negligible → yellow and red: high concentration). Most PMS ions exist in the ice grain boundaries, whereas there are almost none in ice crystals. The FFA mapping image of the frozen FFA solution was also obtained based on its characteristic Raman peak (C = C stretching mode) intensity at 1504 cm^{-1} [56] under excitation at 532 nm (Fig. 5d). The spatial distribution of FFA in the frozen sample (red, yellow, and green colors in the ice grain boundaries and black and violet colors in the ice crystals) clearly indicates that FFA is also highly concentrated in the ice grain boundary region after freezing.

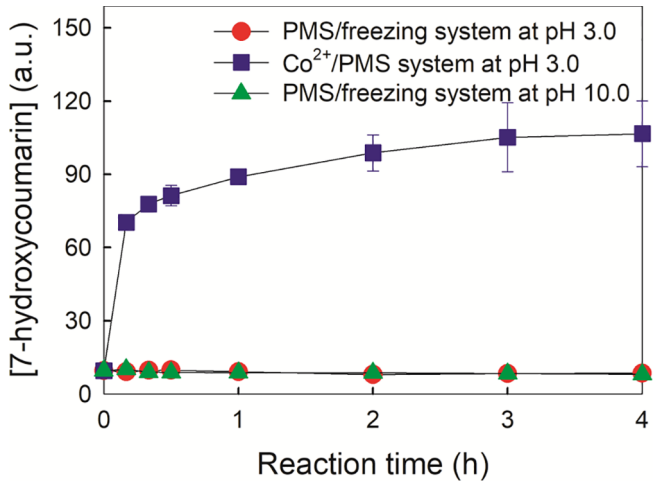

Fig. 4. Production of 7-hydroxycoumarin in the presence of coumarin in the PMS/freezing system and the Co^{2+}/PMS system. Experimental conditions: [PMS] = 100 μM, [FFA] = 20 μM, [Co^{2+}] = 20 μM for the Co^{2+}/PMS system, [coumarin] = 1 mM, pH 3.0 or 10.0, and reaction temperatures = 25 °C for the Co^{2+}/PMS system and −20 °C for the PMS/freezing system.

To establish the concentration effect of PMS on the degradation of FFA, the degradation kinetics of FFA in aqueous solution was measured with increasing PMS concentration from 10 μM to 100 mM (Fig. 6). The degradation of FFA proceeded more rapidly with increasing PMS concentration (Fig. 6a). The degradation rate constant of FFA (k), calculated according to a pseudo-first-order equation, increased in proportional to PMS concentration (r^2 = 0.984) (Fig. 6b). This result indicates that the degradation rate has a close relationship to PMS concentration. Based on the results of Fig. 5c and 6, it can be concluded that the accumulation of PMS in the ice grain boundaries is responsible for the accelerated degradation of FFA in frozen solution. In addition, the increased concentration of FFA in the ice grain boundaries during freezing (Fig. 5d) should have a synergistic effect on the PMS-mediated degradation of FFA by increasing the chance of collision between PMS and FFA.

A few studies reported that the chemical reactions in frozen solution were accelerated because the ice crystals served as a catalytic surface [57–59], which reduces the activation energy for chemical reactions. However, the degradation of FFA by PMS in aqueous solution was negligible even in the presence of ice pellets (Fig. 7). This result can rule out the possibility that the catalytic effect of ice crystals may accelerate the PMS-mediated degradation of FFA in frozen solution.

3.3. PMS-mediated degradation of FFA in frozen solution under various conditions

The effect of PMS concentration, initial pH (aqueous solution pH before freezing), and freezing temperature on the PMS-mediated degradation of FFA in frozen solution was investigated to determine the optimal conditions of the PMS/freezing system (Fig. 8). It should be noted that the degradation rate (pseudo-first-order degradation rate constant, k) in Fig. 8 inset should be taken only as a rough estimate because the degradation of FFA is initiated after the aqueous sample is almost completely frozen (i.e., an induction period for FFA degradation exists). The k value of FFA increased with increasing PMS concentration (Fig. 8a). To be more concrete, the k value linearly increased at [PMS] ≤ 100 μM, but slowly increased at [PMS] ≥ 100 μM. Therefore, the excessive use of PMS is not desirable in the PMS/freezing system for the degradation of aquatic pollutants.

Fig. 8b and c show the degradation kinetics of FFA in the presence of PMS in aqueous and ice phases depending on the initial pH. The PMS-mediated degradation of FFA was negligible in aqueous solution

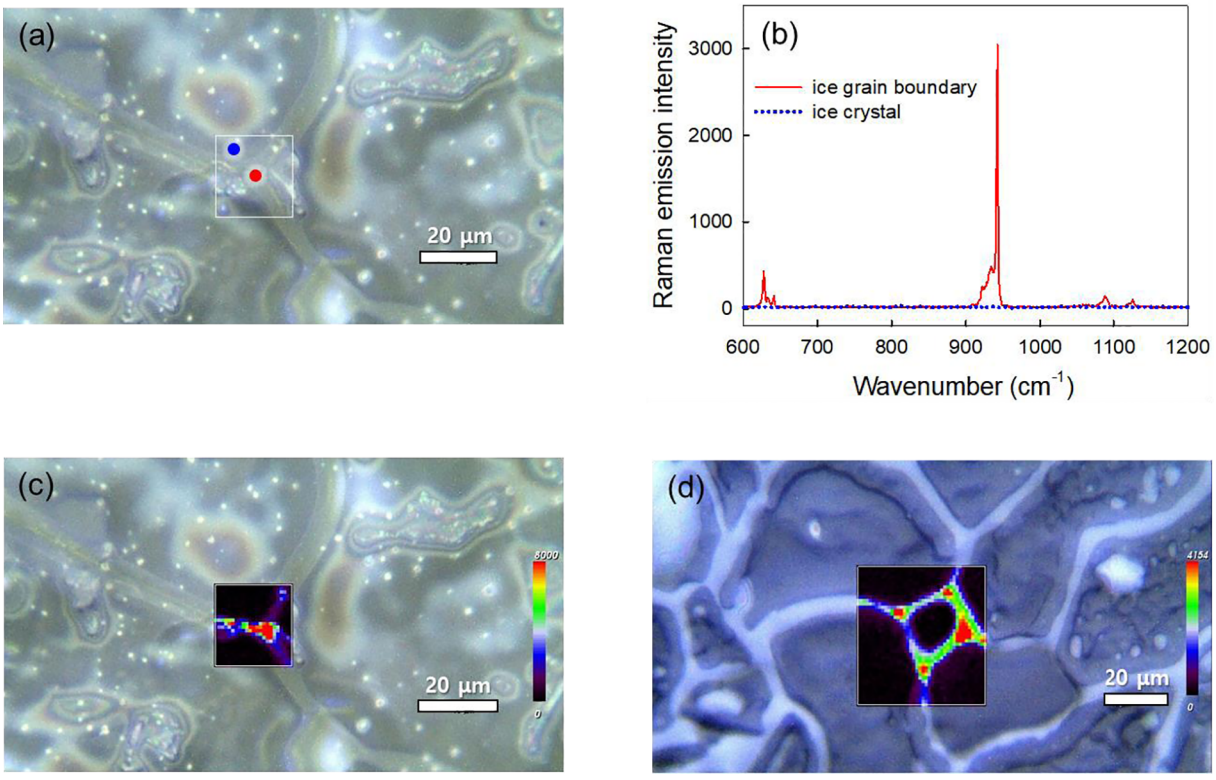

Fig. 5. (a) Optical image of the frozen PMS solution. (b) Raman spectra of PMS in the ice grain boundary (site marked with red circle in a) and ice crystal (site marked with blue circle in a). Spatial distributions of (c) PMS and (d) FFA in the frozen PMS and FFA solutions, respectively. Experimental conditions: [PMS] = 100 μM (for parts a, b, and c), [FFA] = 10 mM (for part d), pH 3.0, and freezing temperature = decrease from 0 to −20 °C at a rate of −1.5 °C/min.

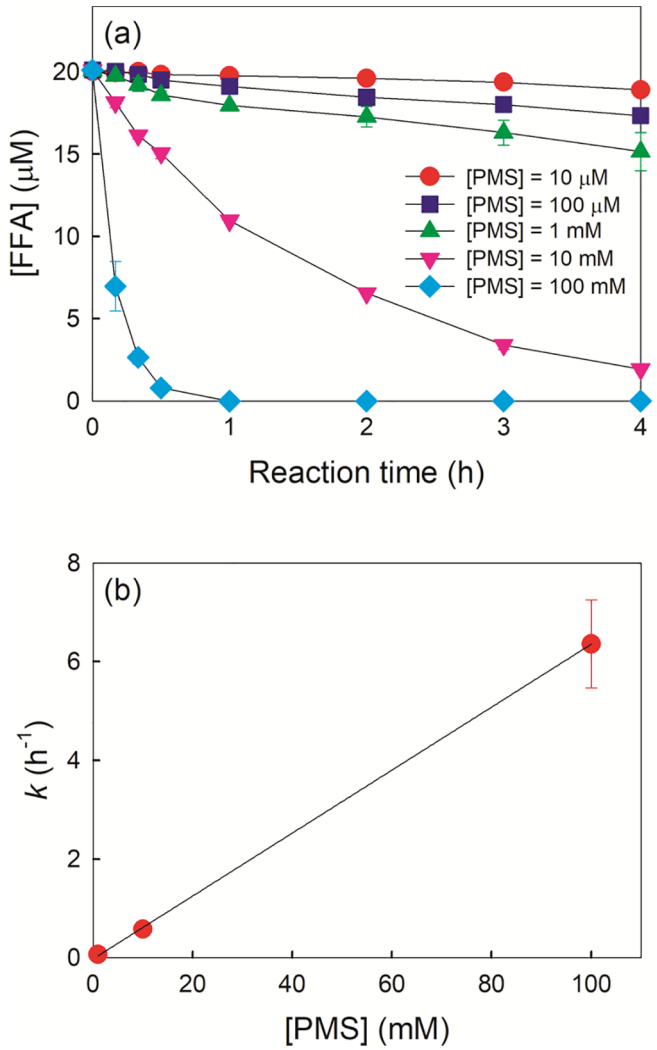

Fig. 6. (a) Effect of initial PMS concentration on the degradation of FFA in aqueous solution. (b) Relationship between initial PMS concentration and pseudo-first-order degradation rate constant (k) of FFA. Experimental conditions: [FFA] = 20 μM, pH 3.0, and reaction temperature = 25 °C for aqueous phase reactions.

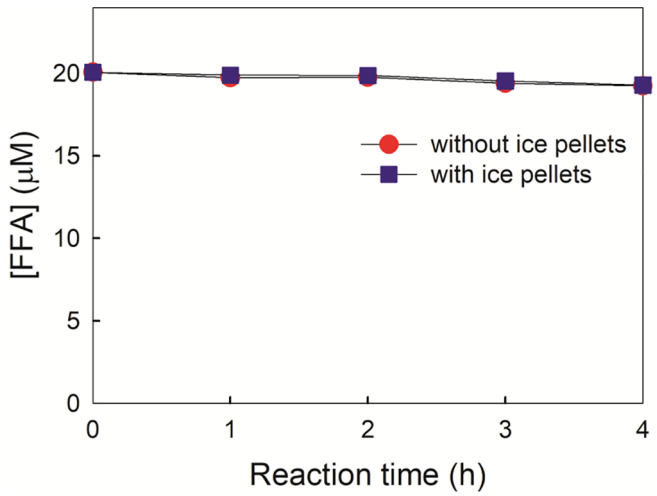

Fig. 7. Degradation of FFA by PMS in aqueous solution in the absence and presence of ice pellets. Experimental conditions: [PMS] = 100 μM, [FFA] = 20 μM, pH 3.0, and reaction temperature = 4 °C for aqueous phase reactions.

(Fig. 8b), whereas it was significant in frozen solution in the pH range of 3–10 (Fig. 8c). The degradation of FFA by PMS in frozen solution was complete within 3 h at all pH values tested. Importantly, the initial pH did not significantly affect the degradation rate of FFA in frozen solution (k values = 1.7–2.2). It has been reported that the degradation efficiency depends on the solution pH in radical-mediated oxidation processes, because $SO_4^{\cdot -}$ and $^{\cdot}OH$ dominantly exist under acidic and basic conditions respectively, and the reactivity of radical species toward pollutants varies depending on the type of radical species [3]. The similar degradation efficiency of the PMS/freezing system over a wide range of pH supports that radicals are little involved in the degradation process. Because the direct electron transfer from organic pollutants to PMS (non-radical mechanism) is the primary degradation pathway in the PMS/freezing system, the effect of pH on the degradation rate is minor in the PMS/freezing system.

The degradation capacity of the previous PMS activation systems, such as carbon nanotubes [16], noble metal nanoparticles [15], bases [60], and phosphates [61], is highly pH-sensitive. Such pH-dependent degradation efficiency inherently limits the utilization of PMS for water treatment. The degradation rate of pollutants in the freezing-induced water treatment systems previously reported was also dependent on the initial pH and negligible under neutral and basic conditions [24–27]. In this regard, the wide working pH range of the PMS/freezing system clearly makes it a more practical water treatment method than the pH-sensitive PMS activation systems and the previous freezing-induced water treatment systems.

The degradation of FFA by PMS in frozen solution was also measured as a function of the freezing temperature (Fig. 8d). Complete degradation was observed at all freezing temperatures tested (−10 to −35 °C). The degradation of FFA in frozen solution proceeded more rapidly at lower freezing temperatures (i.e., the k value increased as the temperature decreased). The accumulation rate of PMS and FFA in the ice grain boundaries should increase with decreasing freezing temperature because ice crystals grow faster and, at the same time, ice grain boundary regions decline faster at lower freezing temperatures. Higher concentrations of PMS and FFA in the smaller ice grain boundaries at lower freezing temperatures provide a better condition for the redox chemical reaction between PMS and FFA. This freezing temperature-dependent concentration effect can help explain why the degradation rate is in inverse proportion to the freezing temperature. However, it should be noted that the times required for completely degrading FFA were not significantly different in the temperature range of −10 to −35 °C. On the other hand, the energy costs for freezing sharply increase with decreasing freezing temperature. Therefore, the operation of the PMS/freezing system at higher freezing temperatures would be more cost-effective.

3.4. Practical viability of the PMS/freezing system for water treatment

To verify the practical viability of the PMS/freezing system for water treatment, the degradation kinetics of various organic pollutants, such as phenol, bisphenol A, 4-methylphenol, propranolol, sulfamoxole, tryptophan, and sulfamethoxazole, in frozen solution were measured and compared with those in aqueous solution (Fig. 9). Although the degradation rate of organic pollutants in the PMS/freezing system was greatly dependent on the type of organic pollutants, the degradation of all organic pollutants tested was enhanced by freezing. In particular, the degradation of pharmaceutical pollutants such as propranolol, sulfamoxole, tryptophan, and sulfamethoxazole proceeded more rapidly than phenolic pollutants such as phenol, 4-methylphenol, and bisphenol A. This highly pollutant-dependent degradation efficiency reconfirms that $SO_4^{\cdot -}$ (non-selective oxidant) is negligibly involved in the degradation processes in the PMS/freezing system. For example, although phenol ($k = 8.8 \times 10^9\ M^{-1}\ s^{-1}$) [43] is more reactive than tryptophan ($k = 2.0 \times 10^9\ M^{-1}\ s^{-1}$) [62] toward $SO_4^{\cdot -}$, tryptophan was more rapidly degraded compared to phenol in the PMS/freezing

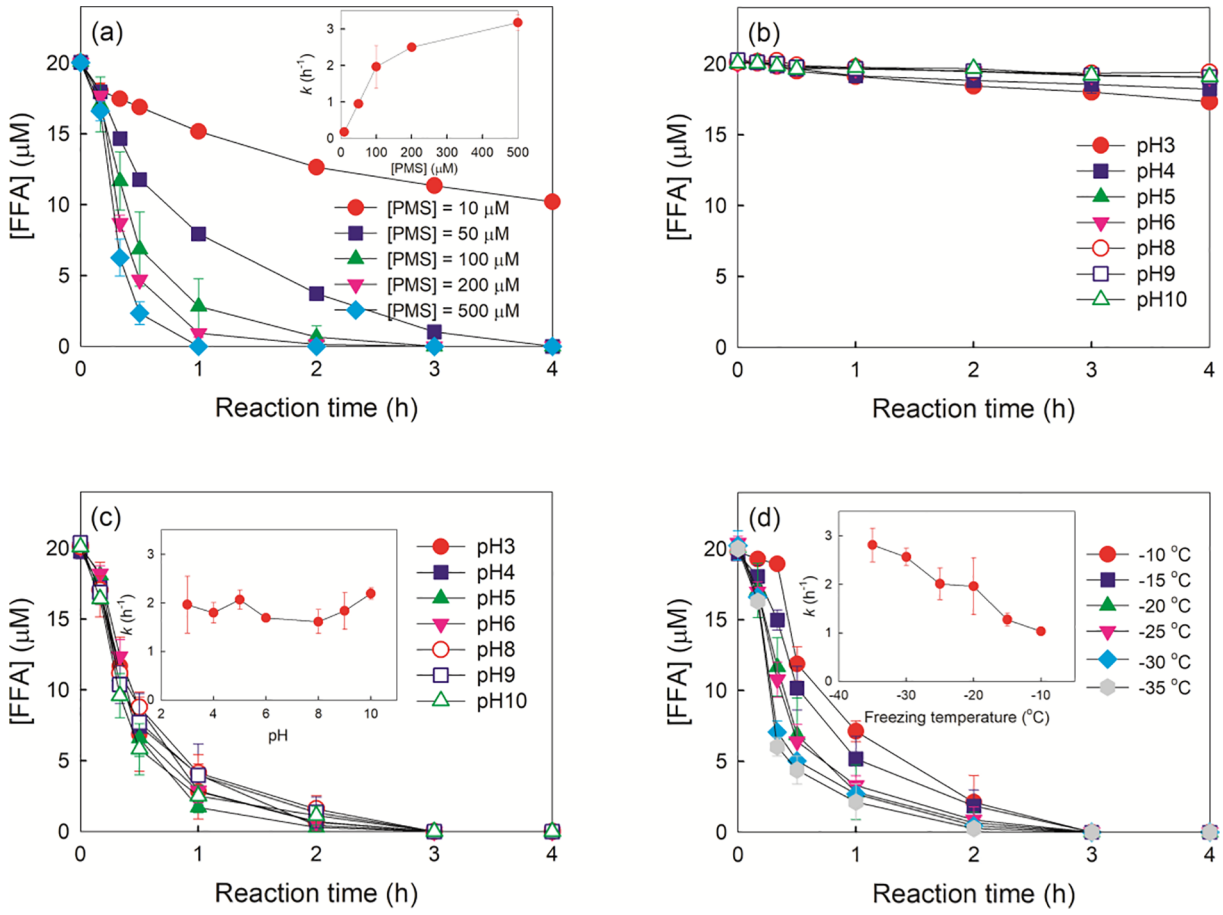

Fig. 8. (a) Effect of PMS concentration on the degradation of FFA in frozen solution. Initial pH-dependent degradation of FFA in (b) aqueous and (c) frozen solutions. (d) Freezing temperature-dependent degradation of FFA in frozen solution. Experimental conditions: [PMS] = 100 μM (for parts b, c, and d), [FFA] = 20 μM, pH 3.0 (for parts a and d), and reaction temperatures = 25 °C for aqueous phase reactions (for part b) and −20 °C for ice phase reactions (for parts a and c).

system. Therefore, the different reactivity of PMS depending on the type of pollutants in frozen solution should be due to the different affinities of pollutants toward PMS because the direct electron transfer process (non-radical mechanism) essentially requires contact between two species. The application of the PMS/freezing system may be restricted to specific pollutants. However, the selective oxidation property of the PMS/freezing system prevents PMS from reacting with background species, which reduces the dose of PMS and enhances the degradation efficiency of target pollutants.

Fig. 10 shows the repeated runs of tryptophan degradation in the PMS/freezing system. The aqueous solution containing PMS (100 μM) and tryptophan (20 μM) was frozen for 30 min, the frozen sample was thawed, and then tryptophan (20 μM) was newly injected prior to refreezing. The injection of tryptophan was repeated at the beginning of each cycle. When PMS was added only at the beginning of first freezing cycle, the degradation efficiency of tryptophan was gradually reduced as the freezing cycle was repeated (1st freezing cycle: 98%, 2nd freezing cycle: 89%, 3rd freezing cycle: 45%, 4th freezing cycle: 7%, and 5th freezing cycle: 1%), which is primarily ascribed to PMS depletion (conversion to SO_4^{2-}). However, the degradation of tryptophan was nearly complete in all freezing cycles when PMS (100 μM) was repeatedly injected at the beginning of odd-numbered freezing cycles. The regular injection of PMS in the course of the freeze/thaw cycling process maintains a constant degradation efficiency, which makes the PMS/freezing system practically feasible for water treatment.

It should be noted that because the degradation in the PMS/freezing system primarily proceeds through the non-radical mechanism, the consumption of PMS is stopped or significantly reduced after the complete degradation of target pollutants. This behavior allows for the reuse of residual PMS and minimizes the chemical cost for water treatment. Nonetheless, if the PMS/freezing system is operated using external (electrical) energy, it may not be economical to treat a large volume of wastewater because a lot of energy is expended to freeze the whole wastewater. However, the PMS/freezing system can achieve water treatment without external energy in cold regions such as polar regions, high latitudes, and midlatitudes during the winter season. The temperatures of these regions frequently drop below −10 °C [63,64], at which the PMS/freezing system works efficiently. Therefore, the PMS/freezing system for water treatment would be economically feasible in cold regions. The material and design of the reactor should be important factors in determining the degradation rate and efficiency in the PMS/freezing system. Therefore, these factors should be considered in the manufacture of reactor. Furthermore, the degradation experiments in various types of reactors with different shapes, volumes, and materials need to be performed and compared.

4. Conclusions

We investigated the degradation of aquatic organic pollutants by PMS in frozen solution at −20 °C compared with that in aqueous

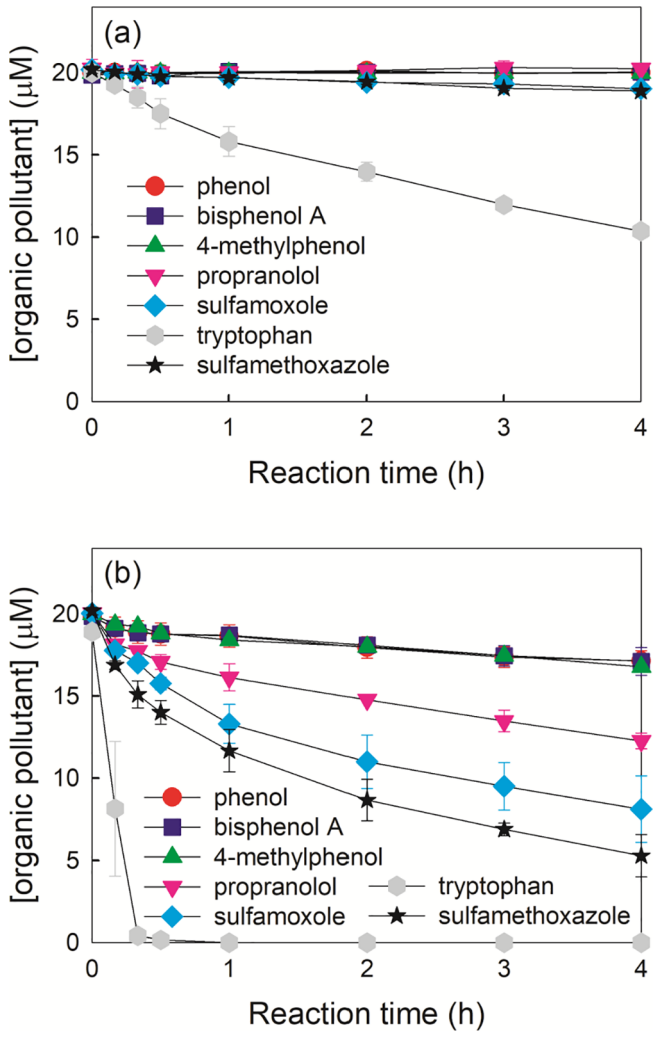

Fig. 9. Degradation of various organic pollutants by PMS in (a) aqueous and (b) frozen solutions. Experimental conditions: [PMS] = 100 μM, [organic pollutant] = 20 μM, pH 3.0, and reaction temperatures = 25 °C for aqueous phase reactions (for part a) and −20 °C for ice phase reactions (for part b).

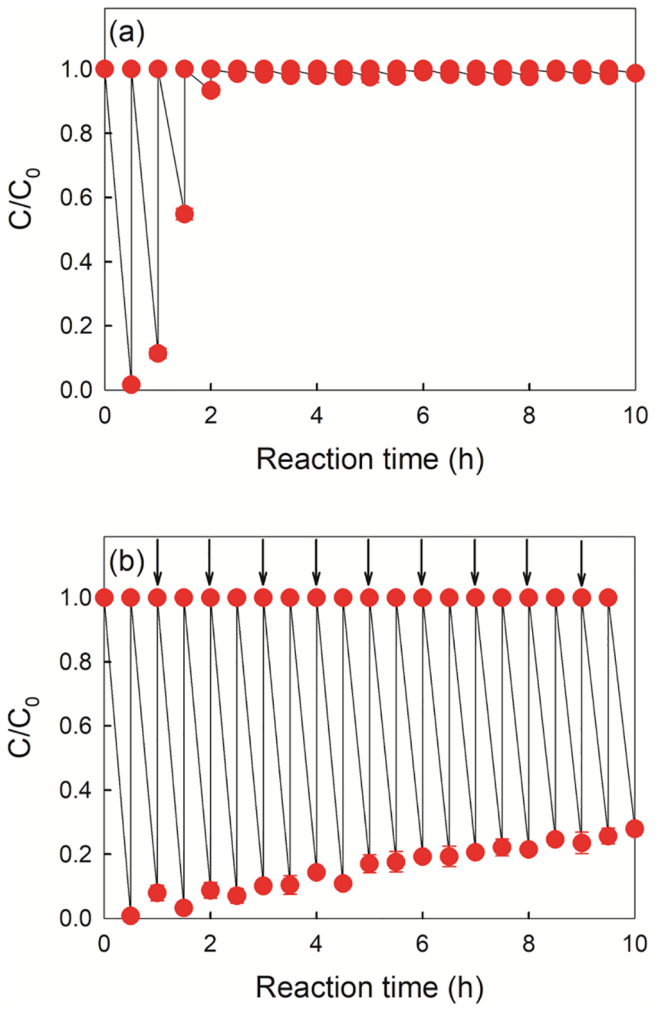

Fig. 10. Repeated runs of tryptophan degradation in the PMS/freezing system with (a) a single injection of PMS and (b) regular injections of PMS as indicated by arrows. Experimental conditions: initial [PMS] = 100 μM, injected [PMS] = 100 μM (for part b), initial and injected [tryptophan] = 20 μM, pH 3.0, and reaction temperature = −20 °C for ice phase reactions.

solution at 25 °C. The degradation of all organic pollutants tested in the presence of PMS was accelerated by freezing. The enhanced degradation in frozen solution should be attributed to the freeze-concentration effect, that accumulates PMS and organic pollutants in the ice grain boundaries and increases their collision frequency. This behavior kinetically accelerates the direct two-electron transfer from organic pollutants to PMS (i.e., the simultaneous oxidation of organic pollutants and the reduction of PMS to SO_4^{2-}).

In comparison with the freezing-induced water treatment systems previously reported [24–27], the PMS/freezing system is better both from environmental and practical points of view because the degradation efficiency of the PMS/freezing system is stable over a wide range of pH, and SO_4^{2-} generated from PMS reduction is practically inert. Nanomaterials (or transition metal ions)-induced PMS activation systems require a follow-up separation process to remove nanomaterials (or transition metal ions); however, the PMS/freezing system does not need any physical post-treatments. In addition, in contrast to energy (heat, ultrasound, and UV light)-induced PMS activation systems, the PMS/freezing system can be used for water treatment without external energy in cold regions. With these features, the PMS/freezing system can be proposed as an eco-friendly and practical water treatment method, especially for the degradation of pharmaceutical pollutants such as propranolol, sulfamoxole, tryptophan, and sulfamethoxazole.

Declaration of Competing Interest

The authors declare that they have no known competing financial interests or personal relationships that could have appeared to influence the work reported in this paper.

Acknowledgements

This research was supported by the Korea Polar Research Institute (KOPRI) project (PE20030) and Young Research Program (NRF-2019R1C1C1004640) through the National Research Foundation of Korea (NRF) funded by the Ministry of Science and ICT.

References

[1] G. Lente, J. Kalmár, Z. Baranyai, A. Kun, I. Kék, D. Bajusz, M. Takács, L. Veres, I. Fábián, One- versus two-electron oxidation with peroxomonosulfate ion: reactions with iron(II), vanadium(IV), halide ions, and photoreaction with cerium(III), Inorg. Chem. 48 (2009) 1763–1773.
[2] M. Spiro, The standard potential of the peroxosulphate/sulphate couple, Electrochim. Acta 24 (1979) 313–314.
[3] J. Wang, S. Wang, Activation of persulfate (PS) and peroxymonosulfate (PMS) and application for the degradation of emerging contaminants, Chem. Eng. J. 334 (2018) 1502–1517.
[4] W.H. Koppenol, J.F. Liebman, The oxidizing nature of the hydroxyl radical. A comparison with the ferryl ion (FeO^{2+}), J. Phys. Chem. 88 (1984) 99–101.

[5] R.E. Huie, C.L. Clifton, P. Neta, Electron transfer reaction rates and equilibria of the carbonate and sulfate radical anions, Radiat. Phys. Chem. 38 (1991) 477–481.
[6] M.S. Kim, K.-M. Lee, H.-E. Kim, H.-J. Lee, C. Lee, C. Lee, Disintegration of waste activated sludge by thermally-activated persulfates for enhanced dewaterability, Environ. Sci. Technol. 50 (2016) 7106–7115.
[7] R. Yin, W. Guo, H. Wang, J. Du, X. Zhou, Q. Wu, H. Zheng, J. Chang, N. Ren, Enhanced peroxymonosulfate activation for sulfamethazine degradation by ultrasound irradiation: performances and mechanisms, Chem. Eng. J. 335 (2018) 145–153.
[8] C. Cui, L. Jin, L. Jiang, Q. Han, K. Lin, S. Lu, D. Zhang, G. Cao, Removal of trace level amounts of twelve sulfonamides from drinking water by UV-activated peroxymonosulfate, Sci. Total Environ. 572 (2016) 244–251.
[9] Y.-H. Guan, J. Ma, X.-C. Li, J.-Y. Fang, L.-W. Chen, Influence of pH on the formation of sulfate and hydroxyl radicals in the UV/peroxymonosulfate system, Environ. Sci. Technol. 45 (2011) 9308–9314.
[10] G.P. Anipsitakis, D.D. Dionysiou, Degradation of organic contaminants in water with sulfate radicals generated by the conjunction of peroxymonosulfate with cobalt, Environ. Sci. Technol. 37 (2003) 4790–4797.
[11] G.P. Anipsitakis, D.D. Dionysiou, Radical generation by the interaction of transition metals with common oxidants, Environ. Sci. Technol. 38 (2004) 3705–3712.
[12] G.-X. Huang, C.-Y. Wang, C.-W. Yang, P.-C. Guo, H.-Q. Yu, Degradation of bisphenol A by peroxymonosulfate catalytically activated with $Mn_{1.8}Fe_{1.2}O_4$ nanospheres: synergism between Mn and Fe, Environ. Sci. Technol. 51 (2017) 12611–12618.
[13] J. Li, M. Xu, G. Yao, B. Lai, Enhancement of the degradation of atrazine through $CoFe_2O_4$ activated peroxymonosulfate (PMS) process: kinetic, degradation intermediates, and toxicity evaluation, Chem. Eng. J. 348 (2018) 1012–1024.
[14] J. Lim, J.M. Lee, C. Kim, S.-J. Hwang, J. Lee, W. Choi, Two-dimensional RuO_2 nanosheets as robust catalysts for peroxymonosulfate activation, Environ. Sci.: Nano 6 (2019) 2084–2093.
[15] Y.-Y. Ahn, E.-T. Yun, J.-W. Seo, C. Lee, S.H. Kim, J.-H. Kim, J. Lee, Activation of peroxymonosulfate by surface-loaded noble metal nanoparticles for oxidative degradation of organic compounds, Environ. Sci. Technol. 50 (2016) 10187–10197.
[16] E.-T. Yun, J.H. Lee, J. Kim, H.-D. Park, J. Lee, Identifying the nonradical mechanism in the peroxymonosulfate activation process: singlet oxygenation versus mediated electron transfer, Environ. Sci. Technol. 52 (2018) 7032–7042.
[17] W. Ma, N. Wang, Y. Fan, T. Tong, X. Han, Y. Du, Non-radical-dominated catalytic degradation of bisphenol A by ZIF-67 derived nitrogen-doped carbon nanotubes frameworks in the presence of peroxymonosulfate, Chem. Eng. J. 336 (2018) 721–731.
[18] H. Lee, H.-I. Kim, S. Weon, W. Choi, Y.S. Hwang, J. Seo, C. Lee, J.-H. Kim, Activation of persulfates by graphitized nanodiamonds for removal of organic compounds, Environ. Sci. Technol. 50 (2016) 10134–10142.
[19] T. Bartels-Rausch, H.-W. Jacobi, T.F. Kahan, J.L. Thomas, E.S. Thomson, J.P.D. Abbatt, M. Ammann, J.R. Blackford, H. Bluhm, C. Boxe, F. Domine, M.M. Frey, I. Gladich, M.I. Guzmán, D. Heger, Th. Huthwelker, P. Klán, W.F. Kuhs, M.H. Kuo, S. Maus, S.G. Moussa, V.F. McNeill, J.T. Newberg, J.B.C. Pettersson, M. Roeselová, J.R. Sodeau, A review of air-ice chemical and physical interactions (AICI): liquids, quasi-liquids, and solids in snow, Atmos. Chem. Phys. 14 (2014) 1587–1633.
[20] R. O'Concubhair, J.R. Sodeau, The effect of freezing on reactions with environmental impact, Accounts Chem. Res. 46 (2013) 2716–2724.
[21] D. Heger, J. Jirkovský, P. Klán, Aggregation of methylene blue in frozen aqueous solutions studied by absorption spectroscopy, J. Phys. Chem. A 109 (2005) 6702–6709.
[22] D. Heger, J. Klánová, P. Klán, Enhanced protonation of cresol red in acidic aqueous solutions caused by freezing, J. Phys. Chem. B 110 (2006) 1277–1287.
[23] K. Kim, J. Ju, B. Kim, H.Y. Chung, Ľ. Vetráková, D. Heger, A. Saiz-Lopez, W. Choi, J. Kim, Nitrite-induced activation of iodate into molecular iodine in frozen solution, Environ. Sci. Technol. 53 (2019) 4892–4900.
[24] F. Sun, Y. Xiao, D. Wu, W. Zhu, Y. Zhou, Nitrite-driven abiotic transformation of sulfonamide micropollutants during freezing process, Chem. Eng. J. 327 (2017) 1128–1134.
[25] J. Ju, J. Kim, Ľ. Vetráková, J. Seo, D. Heger, C. Lee, H.-I. Yoon, K. Kim, J. Kim, Accelerated redox reaction between chromate and phenolic pollutants during freezing, J. Hazard. Mater. 329 (2017) 330–338.
[26] F. Sun, K. Xiao, W. Zhu, N. Withanage, Y. Zhou, Enhanced sludge solubilization and dewaterability by synergistic effects of nitrite and freezing, Water Res. 130 (2018) 208–214.
[27] Y. Choi, H.-I. Yoon, C. Lee, Ľ. Vetráková, D. Heger, K. Kim, J. Kim, Activation of periodate by freezing for the degradation of aqueous organic pollutants, Environ. Sci. Technol. 52 (2018) 5378–5385.
[28] G. Hua, D.A. Reckhow, J. Kim, Effect of bromide and iodide ions on the formation and speciation of disinfection byproducts during chlorination, Environ. Sci. Technol. 40 (2006) 3050–3056.
[29] H. Gallard, S. Allard, R. Nicolau, U. von Gunten, J.P. Croué, Formation of iodinated organic compounds by oxidation of iodide-containing waters with manganese dioxide, Environ. Sci. Technol. 43 (2009) 7003–7009.
[30] J. Lim, Y. Yang, M.R. Hoffmann, Activation of peroxymonosulfate by oxygen vacancies-enriched cobalt-doped black TiO_2 nanotubes for the removal of organic pollutants, Environ. Sci. Technol. 53 (2019) 6972–6980.
[31] K.-I. Ishibashi, A. Fujishima, T. Watanabe, K. Hashimoto, Detection of active oxidative species in TiO_2 photocatalysis using the fluorescence technique, Electrochem. Commun. 2 (2000) 207–210.
[32] O. Tomita, T. Otsubo, M. Higashi, B. Ohtani, R. Abe, Partial oxidation of alcohols on visible-light-responsive WO_3 photocatalysts loaded with palladium oxide cocatalyst, ACS Catal. 6 (2016) 1134–1144.
[33] H. Wang, Y. Song, J. Xiong, J. Bi, L. Li, Y. Yu, S. Liang, L. Wu, Highly selective oxidation of furfuryl alcohol over monolayer titanate nanosheet under visible light irradiation, Appl. Catal. B: Environ. 224 (2018) 394–403.
[34] R.M. Moore, O.C. Zafiriou, Photochemical production of methyl iodide in seawater, J. Geophys. Res.: Atmos. 99 (1994) 16415–16420.
[35] G.T.F. Wong, The marine geochemistry of iodine, Rev. Aquat. Sci. 4 (1991) 45–73.
[36] J.R.E. Jones, A study of the relative toxicity of anions, with *Polycelis Nigra* as test animal, J. Exp. Biol. 18 (1941) 170–181.
[37] T.K. Lau, W. Chu, N.J.D. Graham, The aqueous degradation of butylated hydroxyanisole by UV/$S_2O_8^{2-}$: study of reaction mechanisms via dimerization and mineralization, Environ. Sci. Technol. 41 (2007) 613–619.
[38] H. Gimmler, C. Weiss, The effect of sulfate deficiency and excess sulfate on growth and metabolism of *Dunaliella parva*, J. Plant Physiol. 131 (1987) 449–465.
[39] M. Bochenek, G.J. Etherington, A. Koprivova, S.T. Mugford, T.G. Bell, G. Malin, S. Kopriva, Transcriptome analysis of the sulfate deficiency response in the marine microalga *Emiliania huxleyi*, New Phytol. 199 (2013) 650–662.
[40] P. Parpot, A.P. Bettencourt, G. Chamoulaud, K.B. Kokoh, E.M. Belgsir, Electrochemical investigations of the oxidation-reduction of furfural in aqueous medium: application to electrosynthesis, Electrochim. Acta 49 (2004) 397–403.
[41] C.L. Clifton, R.E. Huie, Rate constants for hydrogen abstraction reactions of the sulfate radical, SO_4^{-}. Alcohols, Int. J. Chem. Kinet. 21 (1989) 677–687.
[42] S. Padmaja, Z.B. Alfassi, P. Neta, R.E. Huie, Rate constants for reactions of SO_4^{-} radicals in acetonitrile, Int. J. Chem. Kinet. 25 (1993) 193–198.
[43] J. Ziajka, W. Pasiuk-Bronikowska, Rate constants for atmospheric trace organics scavenging SO_4^{-} in the Fe-catalysed autoxidation of S(IV), Atmos. Environ. 39 (2005) 1431–1438.
[44] P. Neta, V. Madhavan, H. Zemel, R.W. Fessenden, Rate constants and mechanism of reaction of SO_4^{-} with aromatic compounds, J. Am. Chem. Soc. 99 (1977) 163–164.
[45] Z. Wang, R.T. Bush, L.A. Sullivan, C. Chen, J. Liu, Selective oxidation of arsenite by peroxymonosulfate with high utilization efficiency of oxidant, Environ. Sci. Technol. 48 (2014) 3978–3985.
[46] A. Rastogi, S.R. Al-Abed, D.D. Dionysiou, Sulfate radical-based ferrous–peroxymonosulfate oxidative system for PCBs degradation in aqueous and sediment systems, Appl. Catal. B: Environ. 85 (2009) 171–179.
[47] J. Kim, G.-H. Moon, S. Kim, J. Kim, Photocatalytic oxidation mechanism of arsenite on tungsten trioxide under visible light, J. Photochem. Photobiol. A: Chem. 311 (2015) 35–40.
[48] N. Hasan, G.-H. Moon, J. Park, J. Park, J. Kim, Visible light-induced degradation of sulfa drugs on pure TiO_2 through ligand-to-metal charge transfer, Sep. Purif. Technol. 203 (2018) 242–250.
[49] S. Yang, P. Wang, X. Yang, L. Shan, W. Zhang, X. Shao, R. Niu, Degradation efficiencies of azo dye acid orange 7 by the interaction of heat, UV and anions with common oxidants: persulfate, peroxymonosulfate and hydrogen peroxide, J. Hazard. Mater. 179 (2010) 552–558.
[50] E. Hayon, A. Treinin, J. Wilf, Electronic spectra, photochemistry, and autoxidation mechanism of the sulfite-bisulfite-pyrosulfite systems. The SO_2^{-}, SO_3^{-}, SO_4^{-}, and SO_5^{-} radicals, J. Am. Chem. Soc. 94 (1972) 47–57.
[51] G.P. Anipsitakis, D.D. Dionysiou, M.A. Gonzalez, Cobalt-mediated activation of peroxymonosulfate and sulfate radical attack on phenolic compounds. Implications of chloride ions, Environ. Sci. Technol. 40 (2006) 1000–1007.
[52] K.H. Chan, W. Chu, Degradation of atrazine by cobalt-mediated activation of peroxymonosulfate: different cobalt counteranions in homogenous process and cobalt oxide catalysts in photolytic heterogeneous process, Water Res. 43 (2009) 2513–2521.
[53] E.H. Appelman, L.J. Basile, H. Kim, J.R. Ferraro, Molecular vibrational spectra of potassium peroxymonosulfate, $KHSO_5$ and $KHSO_5 \cdot H_2O$, and of the aqueous peroxymonosulfate ion, Spectroc. Acta Part A: Molec. Biomolec. Spectr. 41A (1985) 1295–1300.
[54] Y. Ren, L. Lin, J. Ma, J. Yang, J. Feng, Z. Fan, Sulfate radicals induced from peroxymonosulfate by magnetic ferrospinel MFe_2O_4 (M = Co, Cu, Mn, and Zn) as heterogeneous catalysts in the water, Appl. Catal. B: Environ. 165 (2015) 572–578.
[55] A. Khan, Z. Liao, Y. Liu, A. Jawad, J. Ifthikar, Z. Chen, Synergistic degradation of phenols using peroxymonosulfate activated by CuO-Co_3O_4@MnO_2 nanocatalyst, J. Hazard. Mater. 329 (2017) 262–271.
[56] T. Kim, R.S. Assary, L.A. Curtiss, C.L. Marshall, P.C. Stair, Vibrational properties of levulinic acid and furan derivatives: raman spectroscopy and theoretical calculations, J. Raman Spectrosc. 42 (2011) 2069–2076.
[57] Z.F. Liu, C.K. Siu, J.S. Tse, Catalysis of the reaction HCl + HOCl → H_2O + Cl_2 on an ice surface, Chem. Phys. Lett. 309 (1999) 335–343.
[58] K. Bolton, J.B.C. Pettersson, Ice-catalyzed ionization of hydrochloric acid, J. Am. Chem. Soc. 123 (2001) 7360–7363.
[59] F. Duvernay, T. Chiavassa, F. Borget, J.-P. Aycard, Experimental study of water-ice catalyzed thermal isomerization of cyanamide into carbodiimide: implication for prebiotic chemistry, J. Am. Chem. Soc. 126 (2004) 7772–7773.
[60] C. Qi, X. Liu, J. Ma, C. Lin, X. Li, H. Zhang, Activation of peroxymonosulfate by base: implications for the degradation of organic pollutants, Chemosphere 151 (2016) 280–288.
[61] X. Lou, L. Wu, Y. Guo, C. Chen, Z. Wang, D. Xiao, C. Fang, J. Liu, J. Zhao, S. Lu, Peroxymonosulfate activation by phosphate anion for organics degradation in water, Chemosphere 117 (2014) 582–585.

[62] P. Neta, R.E. Huie, A.B. Ross, Rate constants for reactions of inorganic radicals in aqueous solution, J. Phys. Chem. Ref. Data 17 (1988) 1027–1284.
[63] V.E. Romanovsky, S.L. Smith, H.H. Christiansen, Permafrost thermal state in the polar northern hemisphere during the international polar year 2007–2009: a synthesis, Permafrost Periglacial Process. 21 (2010) 106–116.
[64] B.K. Biskaborn, S.L. Smith, J. Noetzli, H. Matthes, G. Vieira, D.A. Streletskiy, P. Schoeneich, V.E. Romanovsky, A.G. Lewkowicz, A. Abramov, M. Allard, J. Boike, W.L. Cable, H.H. Christiansen, R. Delaloye, B. Diekmann, D. Drozdov, B. Etzelmüller, G. Grosse, M. Guglielmin, T. Ingeman-Nielsen, K. Isaksen, M. Ishikawa, M. Johansson, H. Johannsson, A. Joo, D. Kaverin, A. Kholodov, P. Konstantinov, T. Kröger, C. Lambiel, J.-P. Lanckman, D. Luo, G. Malkova, I. Meiklejohn, N. Moskalenko, M. Oliva, M. Phillips, M. Ramos, A.B.K. Sannel, D. Sergeev, C. Seybold, P. Skryabin, A. Vasiliev, Q. Wu, K. Yoshikawa, M. Zheleznyak, H. Lantuit, Permafrost is warming at a global scale, Nat. Commun. 10 (2019) 264.